JACS
JOURNAL OF THE AMERICAN CHEMICAL SOCIETY
Article
pubs.acs.org/JACS

Intramolecular Insight into Adsorbate–Substrate Interactions via Low-Temperature, Ultrahigh-Vacuum Tip-Enhanced Raman Spectroscopy

Jordan M. Klingsporn,[†,⊥] Nan Jiang,[†,⊥] Eric A. Pozzi,[†] Matthew D. Sonntag,[†] Dhabih Chulhai,[‡] Tamar Seideman,[†] Lasse Jensen,[‡] Mark C. Hersam,*[,†,§] and Richard P. Van Duyne*[,†,∥]

[†]Northwestern University, Department of Chemistry, 2145 Sheridan Road, Evanston, IL 60208, United States
[‡]The Pennsylvania State University, Department of Chemistry, University Park, PA, 16802, United States
[§]Northwestern University, Department of Materials Science and Engineering, 2220 Campus Drive, Evanston, IL 60208, United States
[∥]Northwestern University, Department of Biomedical Engineering, 2145 Sheridan Road, Evanston, IL 60208, United States

Supporting Information

ABSTRACT: Tip-enhanced Raman spectroscopy (TERS) provides chemical information for adsorbates with nanoscale spatial resolution, single-molecule sensitivity, and, when combined with scanning tunneling microscopy (STM), Ångstrom-scale topographic resolution. Performing TERS under ultrahigh-vacuum conditions allows pristine and atomically smooth surfaces to be maintained, while liquid He cooling minimizes surface diffusion of adsorbates across the solid surface, allowing direct STM imaging. Low-temperature TER (LT-TER) spectra differ from room-temperature TER (RT-TER), RT surface-enhanced Raman (SER), and LT-SER spectra because the vibrational lines are narrowed and shifted, revealing additional chemical information about adsorbate–substrate interactions. As an example, we present LT-TER spectra for the rhodamine 6G (R6G)/Ag(111) system that exhibit such unique spectral shifts. The high spectral resolution of LT-TERS provides intramolecular insight in that the shifted modes are associated with the ethylamine moiety of R6G. LT-TERS is a promising approach for unraveling the intricacies of adsorbate–substrate interactions that are inaccessible by other means.

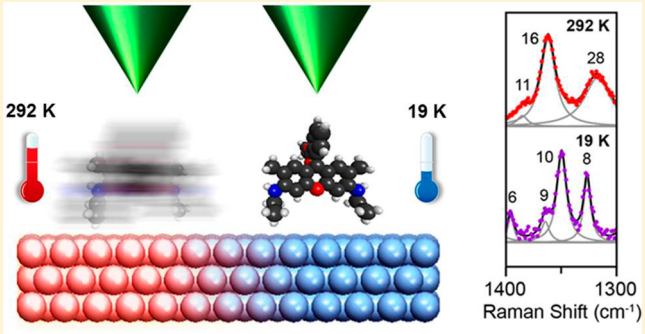

1. INTRODUCTION

Understanding the nature of molecular adsorption geometries and the attendant adsorbate–surface interactions is of fundamental importance in the development of technologies such as dye-sensitized solar cells, organic photovoltaics, heterogeneous catalysts, and molecular electronics. Adsorbate–surface interactions are inherently heterogeneous because of the number of crystallographically distinct surface sites available as well as the various adsorbate–adsorbate interactions possible. Scanning tunneling microscopy (STM) and atomic force microscopy (AFM) provide unprecedented detail about these interactions at the single-molecule (SM) and single-site level for "flat" molecules. Such direct high-resolution imaging is compromised for molecules that have complex 3D adsorption geometries. Tip-enhanced Raman spectroscopy (TERS) is an established tool for surface science that can probe the details of adsorbate–surface interactions for individual molecules adsorbed at individual surface sites.

TERS, unlike surface-enhanced Raman spectroscopy (SERS), utilizes a controllable hot spot formed at the tip–sample junction. This hot spot allows nanofocusing of the electromagnetic (EM) field to provide nanoscale spatial resolution. The high EM field intensity at the tip–sample junction provides enhancements of the Raman signals that are sufficient to provide ultrahigh sensitivity down to the SM level.[1−5] Most of the work in the TERS field has concentrated on studies performed under ambient conditions.[6−10] Performing TERS in ultrahigh vacuum (UHV) can minimize contamination and maximize STM spatial resolution. The first TERS experiment performed in UHV[2] showed SMTER spectra that were dominated by a single vibrational mode for brilliant cresyl blue (BCB) dye molecules deposited from solution on Au(111). The first multivibrational mode UHV-TERS experiment, along with complete UHV sample preparation,[11] was performed for copper phthalocyanine (CuPc) on Ag(111). The recent report of UHV-TERS at 80 K for the *meso*-tetrakis(3,5-di-*tert*-butylphenyl)porphyrin (H2TBPP)/Ag(111) system has further energized this field with its demonstration of sub-

Received: November 27, 2013
Published: February 18, 2014

 © 2014 American Chemical Society dx.doi.org/10.1021/ja411899k | *J. Am. Chem. Soc.* 2014, 136, 3881−3887

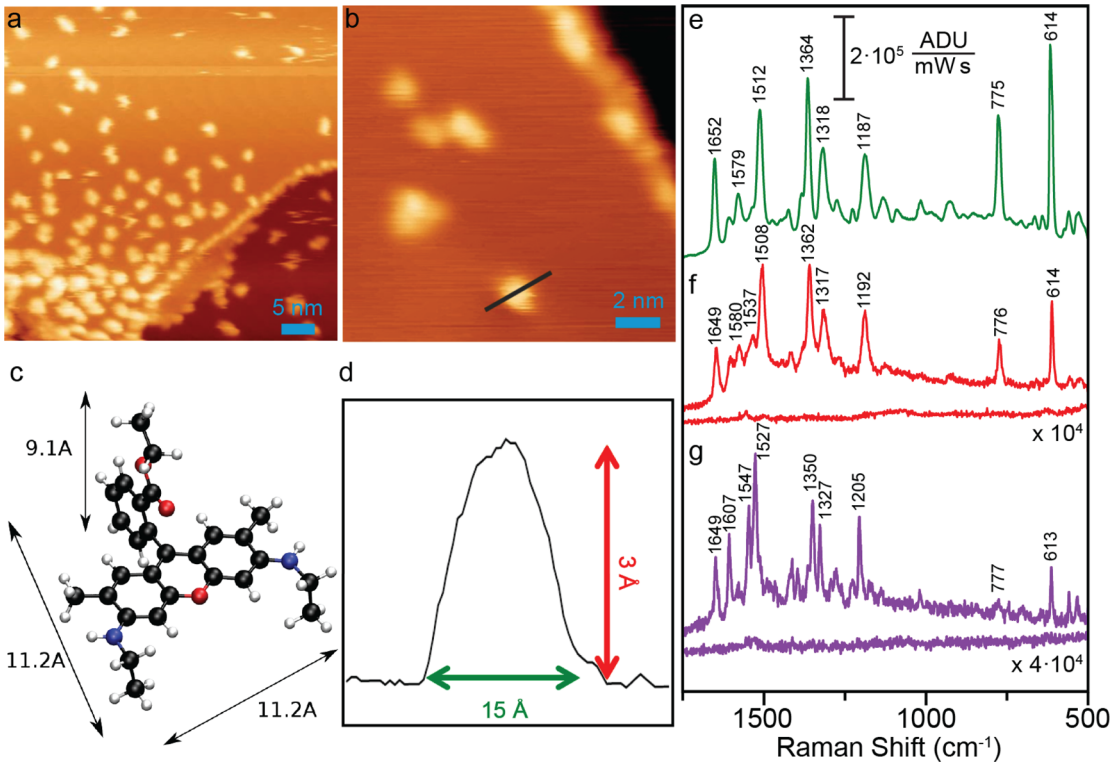

Figure 1. (a) STM topograph of sub-monolayer R6G molecules on a Ag(111) surface measured with a Ag tip. The tip was parked at the lower left corner of the image during the TERS collection (imaging conditions: 2.0 V, 10 pA, 50 nm × 50 nm). (b) Zoom-in STM topograph of individual R6G molecules and clusters (imaging conditions: 2.0 V, 50 pA, 15 nm × 15 nm). (c) Molecular model showing the dimensions of R6G. (d) Line profile across a single R6G molecule. (e) LT-SERS of R6G on an AgFON: λ_{ex} = 532 nm, P_{acq} = 47 μW, t_{acq} = 0.1 s × 100. (f) Engaged and retracted RT-TERS of R6G on Ag(111): λ_{ex} = 532 nm, P_{acq} = 500 μW, t_{acq} = 10 s × 30. (g) Engaged and retracted LT-TERS of R6G on Ag(111): λ_{ex} = 532 nm, P_{acq} = 2 mW, t_{acq} = 60 s.

nanometer spatial resolution.[5] However, the effect of temperature on the TERS signal has not yet been quantified.

Here we present low-temperature (LT) (19 K), UHV (<2 × 10^{-11} Torr) TERS of single molecules and clusters of rhodamine 6G (R6G) adsorbed and immobilized on a Ag(111) surface. Previous LT Raman studies have demonstrated the additional advantage of reduced line widths compared with room temperature (RT), which is evidently dominated by increased vibrational dephasing times.[12−14] Further, a UHV, near-field, variable-temperature SERS study of R6G reported that the background signal narrowed and decreased at LT.[15] We now demonstrate analogous line width narrowing in TERS upon cooling to 19 K as well as informative spectral shifts that are observed in LT-TERS compared with RT-TERS and SERS at both temperatures. Analysis of these spectral shifts using the potential energy distributions (PEDs) of their respective vibrational modes has provided additional information about the specific structural moieties interacting with the Ag(111) surface. This insight has allowed us to postulate a plausible adsorption geometry for R6G on Ag(111). Overall, LT-TERS of a small number of molecules with minimal motional averaging is a significant advance in the study of molecules interacting with surfaces.

2. EXPERIMENTAL SECTION

Sample Preparation. Spectroscopy and imaging were performed with a home-built, cryogenic variable-temperature UHV-STM instrument at a base pressure in the low 10^{-11} Torr range.[11] Clean Ag(111) (Princeton Scientific Corp., one side polished <0.03 μm, orientation accuracy <0.1°) was prepared through several cycles of Ar^+ sputtering and annealing at 700 K. R6G powder ($C_{28}H_{31}N_2O_3Cl$, Aldrich, >99%) was introduced into the UHV chamber in an alumina-coated tungsten filament sublimation module. The powder was degassed prior to deposition via thermal sublimation at 430 K onto Ag(111), which was kept at room temperature (292 K). LT-TERS and STM were performed using liquid He cooling. With the sample and probe in the STM cryostat, liquid He was delivered to the cryostat via a cold finger. Initially, cryostat shutters covering the sapphire windows on either side of the cryostat were kept closed while the sample was brought down to 8 K. The shutters were then opened to allow optical access to the tip−sample junction, leading to a temperature increase due to thermal radiation, and the microscope was allowed to stabilize at 19 K. Illumination of the tip−sample junction using typical experimental parameters showed no measurable increase in the temperature of the sample. STM voltages were applied to the sample with respect to the grounded tip, and images were acquired in constant-current mode.

Tip Preparation. Ag probes were electrochemically etched from 250 μm silver wire (99.9%, Alfa Aesar) under potentiostatic control using the method previously described.[11] Etched probes were rinsed with warm deionized water (Millipore) followed by ethanol and immediately introduced into the UHV chamber for use without further processing.

Spectroscopy. Optics external to the UHV chamber were used for laser (Spectra-Physics, 532 nm) excitation and collection of scattered light (Supporting Information S1). A glass viewport and two sapphire windows afforded optical access to the tip−sample junction. The laser beam was expanded to approximately 25 mm in diameter and focused at the tip−sample junction. Excitation and collection were accomplished through opposing viewports with excitation and collection both centered at approximately 75° with respect to the surface normal. Laser excitation was polarized along the axis of the tip and stabilized (Brockton Electro-Optics Corp.) to minimize intensity fluctuations. A high-resolution witness camera (Uniq, UM-300) was

dx.doi.org/10.1021/ja411899k | J. Am. Chem. Soc. 2014, 136, 3881−3887

utilized to focus the laser at the tip−sample junction in real time. Laser and Rayleigh light were rejected with a long-pass filter, and the remaining Stokes-scattered light was focused onto the 100 μm entrance slit of a 1/3 m imaging spectrograph (Acton SpectraPro 2360i), after which the light was dispersed (1200 grooves/mm grating, 500 nm blaze, centered at 1100 cm^{-1}) onto a thermoelectrically cooled charge-coupled device (Princeton Instruments Pixis 400, 1340 × 400 pixels).

SERS Substrate Fabrication. Surface-enhanced Raman reference spectra were obtained in UHV using Ag film over nanosphere (AgFON) substrates.[16] Silica spheres (320 nm) were drop-cast onto a silicon wafer and coated with a 200 nm layer of Ag. The AgFON was optimized for the highest enhancement with 532 nm excitation.[17] R6G molecules were sublimed as described above, and SER spectra were collected at 292 and 19 K using two separate AgFONs that were both optimized for 532 nm excitation.

Theory. The resonance Raman scattering (RRS) of R6G was simulated using a time-dependent wave packet formalism as previously described.[4,18] Briefly, optimized geometries, normal modes, and excitation energies were obtained at the B3LYP/6-311G* level of theory using NWChem.[19] Vibrational frequencies were scaled by a factor of 0.98. Dimensionless displacements were obtained from three-point numerical differentiation of the excited-state energies along mass-weighted vibrational coordinates.

Normal mode distributions were calculated from mass-weighted normal mode vectors. The molecule was first divided into seven regions (two ethylamine, two methyl, one ethyl ester, one phenyl, and one xanthene). The vibrational PEDs were then determined by considering the magnitudes of the normal mode vectors and the regions to which the corresponding atoms belong.

3. RESULTS AND DISCUSSION

Scanning Tunneling Microscopy. Rhodamine 6G is an ionic species and is therefore in a class of molecules rarely used for UHV deposition.[20] Electrospray ion beam deposition (ES-IBD) at the appropriate energies can deposit R6G molecules or molecular fragments onto surfaces in UHV.[21] In the present work, we achieved the successful thermal sublimation of R6G onto a Ag(111) substrate at a pressure of 2×10^{-11} Torr. At RT (292 K), R6G molecules diffuse on the terraces of the Ag(111) surface. STM images at this temperature could not resolve individual adsorbed molecules.[22] Instead, only random noise was detected, revealing the weak adsorption of R6G on the Ag(111) substrate.[23]

Liquid He cooling of the sample to 19 K immobilized the R6G molecules on the surface. Figure 1a,b shows representative STM images of low-coverage R6G on Ag(111) at 19 K. A disordered arrangement of R6G molecules on the Ag(111) surface was observed as a result of deposition at a surface temperature of 292 K. As depicted in Figure 1b, the step edges of the Ag(111) surface were decorated with R6G molecules, which were stable during scanning. However, some molecules on the terrace were dragged along the surface by the STM tip. This is due to the weak interaction between the molecules and the substrate even at 19 K. Individual molecules and clusters were observed by STM on the terraces without any formation of a periodic molecular superlattice. Most of the R6G molecules appeared to form dimers, trimers, or even larger aggregates, indicating that there are attractive interactions between the molecules on the Ag(111) surface. Figure 1d shows a line profile across an R6G monomer on the surface. The width is approximately 15 Å, which agrees with the size of the R6G model (Figure 1c). However, comparison of possible R6G structural model orientations with STM constant-current images did not allow for orientational discrimination, as intramolecular features were not discernible. Therefore, STM topography alone cannot identify the adsorption configuration and conformation of R6G molecules on the Ag(111) surface.

Comparison of Spectral Features in RT/LT-TERS with RT/LT-SERS. Because of the limited information given by LT-STM, we turned to spectroscopy in order to elucidate the nature of the adsorbate−substrate interactions. Figure 1e−g depicts LT-SERS and both RT- and LT-TERS of R6G. Several differences between LT-TERS and the other spectra can be clearly observed. These differences permit some adsorbate−surface structural properties to be deduced. The focus will be on the following: (1) the number of molecules observed; (2) the Raman line shape; (3) the temperature-dependent Raman line width; and (4) the unique spectral shifts observed only in LT-TERS.

Number of Molecules Observed. In contrast to the TER spectra, the SER spectra contain contributions from all of the molecules within the laser probe volume, resulting in a highly ensemble-averaged signal. On the other hand, the TERS signal is due only to molecules within the TERS enhancing region. The exact size of this enhancing region has been under debate in the literature but is certainly smaller than the probe area in SERS because of nanofocusing of light at the tip apex. Using the previously reported laser focal spot size for this instrument and the estimated coverage from the STM image of similarly deposited R6G in Figure 1a, we approximate that 10^9 molecules are probed in SERS.[11] In contrast, if a typical etched Ag probe morphology and a radius of the TERS enhancing region equal to half of the radius of the probe are assumed,[24] the TERS signal originates from no more than 10^4 R6G molecules. However, as shown with SERS, a few molecules in the region of highest field strength (viz., the hot spot) will dominate the signal.[25] Under this assumption, the lower bound for the number of R6G molecules in the TERS enhancing region would be only a few molecules. Because of the roughness of the SERS substrate, molecules experience many adsorption sites and configurations. Given that varied geometries result in a normal distribution of mode frequencies, the observed broad, Gaussian-shaped bands in SER spectra collected at both temperatures (Figure 2) substantiate this claim.

Raman Line Shape. RT-TERS of R6G drastically reduces the number of molecules in comparison to SERS. However, because R6G rapidly diffuses at RT, motional averaging occurs as molecules move in and out of the TERS enhancing region. Additionally, R6G molecules in TER spectra were adsorbed to an atomically smooth Ag(111) surface, which can be ideally treated as a two-dimensional array of equivalent surface sites. While multiple geometries may exist, the surface uniformity decreases the number of available adsorption conformations. Together, these effects slightly decrease the observed average RT-TERS line width to 17 cm^{-1}, compared with 20 cm^{-1} for RT-SERS (Figure 2 and Supporting Information S2−S4). Consistent with a lesser degree of inhomogeneous broadening, the peaks in RT-TERS were found to be well-fit by a Lorentzian line shape.

Temperature-Dependent Raman Line Width. More significantly, further line narrowing was achieved by conducting the experiments at 19 K. Although the probe area is identical for TERS at the two temperatures, molecules in the RT case are mobile on the surface. During spectral acquisitions, molecules diffuse past differing surface sites and potentially also change their conformation. Consequently, more molecules are probed at RT, and motional averaging causes a distribution in the frequency of a given vibrational mode. We expect this

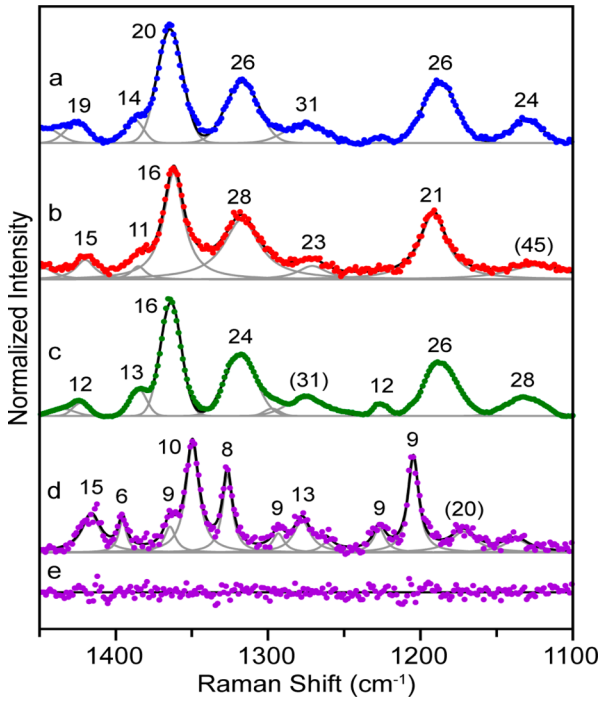

Figure 2. (a) RT-SER, (b) RT-TER, (c) LT-SER, and (d) LT-TER spectra of R6G. The displayed values are full widths at half-maximum (FWHMs) for the corresponding peaks. Spectra were background-subtracted and fit with Gaussians (SERS) or Lorentzians (TERS) using a least-squares approach. Data are represented by colored circles, individual peak fits by gray lines, and composite fits by black lines. (e) Residuals after fitting for LT-TERS. All of the spectra were normalized by the maximum intensity in their respective composite fits. FWHM values in parentheses designate peaks either marginally above 3× noise and/or those largely influenced by background uncertainty.

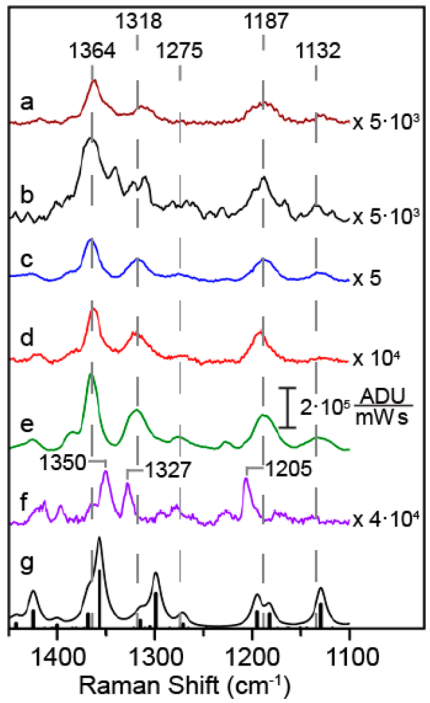

Figure 3. Spectral comparisons for R6G on silver surfaces: (a) ambient SM RT-SERS on Ag colloids (brown), (b) ambient SM RT-TERS on a smooth Ag film (black), (c) RT-UHV-SERS on AgFON (blue), (d) RT-UHV-TERS on Ag(111) (red), (e) LT-UHV-SERS on AgFON (green), (f) LT-UHV-TERS on Ag(111) (violet), and (g) TD-DFT-calculated Raman spectrum of free R6G for the 1450 to 1100 cm^{-1} region. All of the spectra are background-subtracted. The ambient SM TERS spectrum has been smoothed.

inhomogeneous broadening to factor into any single-molecule vibrational spectrum of mobile species as well.[4] This expectation is corroborated in Figures 3 and 4, as previously reported SMSERS and SMTERS do not exhibit line narrowing.[4,26]

In contrast, molecules are immobilized during LT-TERS and experience constant adsorption configurations. In addition, we expect that the stationary molecules adopt one of a finite number of local minimum-energy configurations on the periodic substrate. As a result, the distribution of adsorption geometries and therefore individual mode frequencies is decreased, such that LT-TERS peaks are well-fit by Lorentzian curves and narrowed by nearly 50% to an average line width of 9 cm^{-1} (Figure 2). In some instances, an instrumentally limited line width of 6 cm^{-1} is observed (Supporting Information S5). In contrast, the average line width for LT-SERS was 18 cm^{-1}.

It is appropriate to consider the mechanisms that contribute to the observed line narrowing in LT-TERS. Beyond reduced inhomogeneous broadening, additional narrowing in LT-TERS is afforded through the intrinsic temperature dependence of the Raman line width. It has been shown that SMSERS line widths are temperature-dependent through anharmonic coupling between the molecular vibrations of the adsorbate and the phonons of the silver surface, resulting in an increase in the vibrational dephasing relaxation time.[12] We indeed observe peak narrowing at LT in both TERS and SERS, consistent with these earlier observations, although the effect is significantly more prominent in LT-TERS. It was also shown that pure homogeneously broadened lines in SMSERS have a larger dependence on temperature than inhomogeneously broadened lines (averaged SERS).[12] Accordingly, since the majority of SERS line width broadening is a result of the distribution of surface sites, the variety of potential adsorption configurations, and the large number of sampled molecules, immobilization and increased dephasing times lead to minimal line narrowing in LT-SERS. In contrast, TERS peaks are observed to narrow substantially at LT. An extreme example is the 1327 cm^{-1} LT-TERS peak, which narrowed from 28 to 8 cm^{-1} upon cooling (Figure 2). This degree of narrowing provides additional evidence of low inhomogeneous broadening in LT-TERS, which is made possible through low copy number and immobilization at equivalent surface sites.

Line width narrowing increases the information content available in a collected spectrum. Although there is no standard definition of spectral resolution in Raman spectroscopy,[27] an intuitive one is that in a fixed spectral region the number of resolvable lines increases with decreasing line width. This is clearly observed in Figure 2, in which 12 peaks are resolved in the range 1100−1450 cm^{-1} in LT-TERS compared with eight peaks in RT-TERS.

Unique Spectral Shifts in LT-TERS. Along with the observed line width narrowing, multiple LT-TERS peaks are shifted with respect to both the RT-TER and the RT/LT-SER spectra shown in Figures 3 and 4 (also see Supporting Information S6−S8 for the 500−850 cm^{-1} region, eigenvector diagrams, and TERS at different locations, respectively). Additionally, these figures compare both RT/LT-SER and -TER spectra to previously reported SMTER and SMSER spectra.[4,26] The SM spectra appear to remain consistent with the RT-SER, LT-SER,

dx.doi.org/10.1021/ja411899k | J. Am. Chem. Soc. 2014, 136, 3881−3887

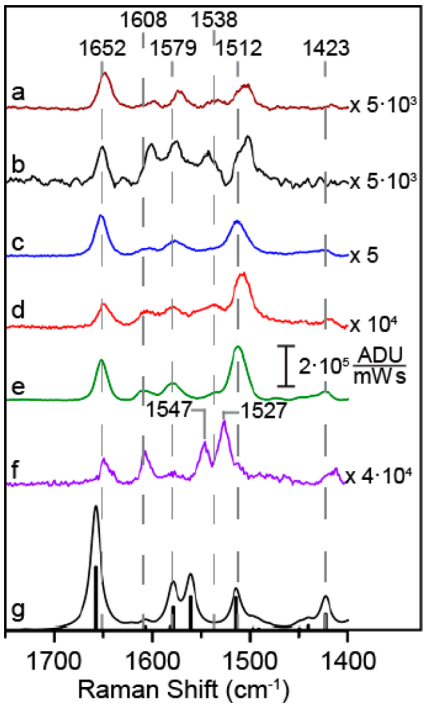

Figure 4. Spectral comparisons for R6G on silver surfaces: (a) ambient SM RT-SERS on Ag colloids (brown), (b) ambient SM RT-TERS on a smooth Ag film (black), (c) RT-UHV-SERS on AgFON (blue), (d) RT-UHV-TERS on Ag(111) (red), (e) LT-UHV-SERS on AgFON (green), (f) LT-UHV-TERS on Ag(111) (violet), and (g) TD-DFT-calculated Raman spectrum of free R6G for the 1750 to 1400 cm^{-1} region. All of the spectra are background-subtracted. The ambient SM TERS spectrum has been smoothed.

and RT-TER spectra but greatly differ from the LT-TER spectra. Both blue and red mode shifts of up to 20 cm^{-1} are observed for multiple LT-TERS modes, while other modes remain unshifted. The unique spectral characteristics observed for LT-TERS combined with a careful theoretical interpretation provide further insight into the molecular orientation of R6G on the Ag(111) surface. Table 1 summarizes the major peaks and indicates whether they are shifted in the LT-TER spectrum, and it also provides the corresponding theoretical PEDs (see Supporting Information S9 for all of the PEDs).

The peaks located at 1132, 1205, 1327, 1350, 1527, and 1547 cm^{-1} in the LT-TER spectrum show frequency shifts compared with both RT/LT-SERS and RT-TERS. As shown by the green boxes in Table 1, all of these peaks have a unique similarity in that each mode is characterized theoretically to have a PED that involves approximately localized vibrations on the ethylamine moieties or on the xanthene ring and ethylamine moieties. For example, the peak observed at 1205 cm^{-1} is shifted with respect to the other spectra and has a PED showing 61% xanthene character and 38% ethylamine character. The modes at 1132, 1327, 1350, 1527, and 1547 cm^{-1} also show large shifts and have PEDs showing large xanthene ring and/or ethylamine character. The rest of the major peaks do not exhibit such shifts. Comparing these unshifted modes with their PED values in Table 1 shows that they have either high phenyl ring character or are highly delocalized modes with contributions from most of the internal coordinates of R6G. An example of an unshifted, phenyl-ring-localized mode is the peak located at 1608 cm^{-1}. The unshifted xanthene-ring-localized mode at 1652 cm^{-1} is worthy of note. This mode only has 1% ethylamine character and is therefore effectively decoupled from the Ag(111) surface. An in-depth discussion of the characteristics of the R6G vibrations will not be presented here, as it has been thoroughly covered previously.[4,26,28]

An alternative explanation for the observed peak shifts might lie in the strength of molecule−molecule interactions. In other words, we consider the possibility that the dimers, trimers, and larger aggregates observed in STM images of R6G on Ag(111) at LT may explain the shifted peaks in LT-TERS. However, since one would expect similar aggregation properties in LT-SERS in this case, the absence of such shifts decreases the likelihood of this scenario. Furthermore, because multiple R6G aggregation states are observed in the STM images, we would expect to see either inhomogeneously broadened or many more peaks in LT-TERS as a result of varying molecule−molecule

Table 1. Major Peaks for LT-TERS[a] and Theoretically Calculated Frequencies and PEDs for the Moieties Present in R6G

Experimental		Theoretical					
Position cm^{-1}	Shifted Y/N	Position cm^{-1}	Methyl %	Xanthene %	Ethylamine %	Phenyl %	Ester %
614	N	616	3.5	39.2	6	51.1	0.1
775	N	772	16.8	42.3	39.7	1.1	0.2
1132	Y	1129	13.5	27.5	40.5	16.1	2.4
1205	Y	1195	0.4	61.2	38.3	0.1	0
1275	N	1271	0.7	70	17.5	9.3	2.5
1327	Y	1321	3.8	11.7	84.4	0	0
1350	Y	1367	0.2	4.7	93.9	1.2	0
1423	N	1424	37.9	30.3	17.1	14.5	0.2
1527	Y	1515	11.8	28.2	58.1	1.8	0.1
1547	Y	1535	6.8	38.6	54.5	0	0
1579	N	1582	0.1	6.9	1.9	90.8	0.4
1608	N	1607	0	3.6	0	96.2	0.2
1652	N	1658	8.9	89.6	1.3	0	0.2

[a]For each peak, the entry in the second column indicates whether the peak is shifted with respect to the other spectra.

dx.doi.org/10.1021/ja411899k | J. Am. Chem. Soc. 2014, 136, 3881−3887

interactions. We thus conclude that intramolecular interactions are not a significant contributor to the peak shifts observed in LT-TERS.

Interpretational Hypothesis and Molecular Orientation. Understanding the unique spectral characteristics observed for LT-TERS in comparison with the other spectra presented here requires an interpretational hypothesis. We hypothesize that the moieties in closest proximity to the surface exhibit the greatest perturbation in the observed Raman frequency. Under this hypothesis, the orientation of R6G on the Ag(111) substrate can be further understood on the basis of the unique spectral characteristics observed.

Using the above hypothesis and the observation that all of the modes localized on the ethylamine moieties or xanthene ring modes coupled to the ethylamine moieties exhibit spectral shifts, we propose that the ethylamine moieties of adsorbed R6G interact with the Ag(111) surface. Therefore, the molecule is likely oriented with the R6G molecule situated edgewise along its xanthene moiety with its ethylamine substituents against the Ag(111) surface.

4. CONCLUSIONS

LT-TERS performed in UHV provides additional insight into the adsorption properties of molecules on surfaces. Upon cooling with liquid He to 19 K, STM imaging revealed that R6G molecules adopt multiple aggregation states, including isolated monomers, at 19 K. Multimodal TER and SER spectra were collected at both RT and LT, and the observed line width and mode frequency differences were analyzed to provide insight into the properties of R6G adsorption and the inherent differences of the techniques. Line widths in LT-TERS were observed to be greatly narrowed with respect to those in all of the other collected spectra because of decreased homogeneous and inhomogeneous broadening. Low copy number and surface homogeneity provide narrowing in TERS relative to SERS, and cooling to LT eliminates motional averaging and increases the vibrational dephasing times. According to the PEDs obtained by time-dependent density functional theory (TD-DFT) calculations on the free R6G molecule, the spectral shifts observed in LT-TERS for certain modes are attributed to their proximity and coupling to the surface. Specifically, we postulate that R6G adsorbs to Ag(111) along its xanthene edge with the ethylamine moieties in close proximity to the surface. Overall, we conclude that LT-TERS enables improved understanding of adsorbate−substrate interactions and thus has the potential to influence the design of future molecular devices.

■ ASSOCIATED CONTENT

Supporting Information

Peak fitting results, calculation results, and instrument information. This material is available free of charge via the Internet at http://pubs.acs.org.

■ AUTHOR INFORMATION

Corresponding Authors

m-hersam@northwestern.edu
vanduyne@northwestern.edu

Author Contributions

⊥J.M.K. and N.J. contributed equally.

Notes

The authors declare no competing financial interest.

■ ACKNOWLEDGMENTS

Primary support was equally provided by the NSF Center for Chemical Innovation dedicated to Chemistry at the Space-Time Limit (CHE-082913) and the Department of Energy, Office of Basic Energy Sciences (DE-FG02-09ER16109). Additional support was provided by the National Science Foundation (CHE-1152547, CHE-0955689, DMR-1121262, and DMR-0520513). E.A.P. acknowledges support from the Hierarchical Materials Cluster Program at NU. This material is based upon work supported by the National Science Foundation Graduate Research Fellowship Program under Grant DGE-1324585.

■ REFERENCES

(1) Zhang, W.; Yeo, B. S.; Schmid, T.; Zenobi, R. *J. Phys. Chem. C* **2007**, *111*, 1733.
(2) Steidtner, J.; Pettinger, B. *Phys. Rev. Lett.* **2008**, *100*, No. 236101.
(3) Liu, Z.; Ding, S.-Y.; Chen, Z.-B.; Wang, X.; Tian, J.-H.; Anema, J. R.; Zhou, X.-S.; Wu, D.-Y.; Mao, B.-W.; Xu, X.; Bing, R.; Tian, Z.-Q. *Nat. Commun.* **2011**, *2*, 305.
(4) Sonntag, M. D.; Klingsporn, J. M.; Garibay, L. K.; Roberts, J. M.; Dieringer, J. A.; Seideman, T.; Scheidt, K. A.; Jensen, L.; Schatz, G. C.; Van Duyne, R. P. *J. Phys. Chem. C* **2012**, *116*, 478.
(5) Zhang, R.; Zhang, Y.; Dong, Z. C.; Jiang, S.; Zhang, C.; Chen, L. G.; Zhang, L.; Liao, Y.; Aizpurua, J.; Luo, Y.; Yang, J. L.; Hou, J. G. *Nature* **2013**, *498*, 82.
(6) Opilik, L.; Bauer, T.; Schmid, T.; Stadler, J.; Zenobi, R. *Phys. Chem. Chem. Phys.* **2011**, *13*, 9978.
(7) Stadler, J.; Schmid, T.; Zenobi, R. *ACS Nano* **2011**, *5*, 8442.
(8) van Schrojenstein Lantman, E. M.; Deckert-Gaudig, T.; Mank, A. J.; Deckert, V.; Weckhuysen, B. M. *Nat. Nanotechnol.* **2012**, *7*, 583.
(9) Hayazawa, N.; Yano, T.; Watanabe, H.; Inouye, Y.; Kawata, S. *Chem. Phys. Lett.* **2003**, *376*, 174.
(10) Domke, K. F.; Zhang, D.; Pettinger, B. *J. Am. Chem. Soc.* **2007**, *129*, 6708.
(11) Jiang, N.; Foley, E. T.; Klingsporn, J. M.; Sonntag, M. D.; Valley, N. A.; Dieringer, J. A.; Seideman, T.; Schatz, G. C.; Hersam, M. C.; Van Duyne, R. P. *Nano Lett.* **2012**, *12*, 5061.
(12) Artur, C.; Le Ru, E. C.; Etchegoin, P. G. *J. Phys. Chem. Lett.* **2011**, *2*, 3002.
(13) Temple, P. A.; Hathaway, C. E. *Phys. Rev. B* **1973**, *7*, 3685.
(14) Tsai, C.-S.; Lin, C.-E.; Lin, J.-C.; Wang, J.-K. *Chem. Phys. Lett.* **1998**, *295*, 509.
(15) Anger, P.; Feltz, A.; Berghaus, T.; Meixner, A. *J. Microsc.* **2003**, *209*, 162.
(16) Hulteen, J. C.; Treichel, D. A.; Smith, M. T.; Duval, M. L.; Jensen, T. R.; Van Duyne, R. P. *J. Phys. Chem. B* **1999**, *103*, 3854.
(17) Greeneltch, N. G.; Blaber, M. G.; Henry, A.-I.; Schatz, G. C.; Van Duyne, R. P. *Anal. Chem.* **2013**, *85*, 2297.
(18) Silverstein, D. W.; Jensen, L. *J. Chem. Phys.* **2012**, *136*, No. 064111.
(19) Bylaska, E.; De Jong, W.; Govind, N.; Kowalski, K.; Straatsma, T.; Valiev, M.; Wang, D.; Apra, E.; Windus, T.; Hammond, J. *NWChem*; Pacific Northwest National Laboratory: Richland, WA, 2007.
(20) Uehara, Y.; Ushioda, S. *Appl. Phys. Lett.* **2005**, *86*, No. 181905.
(21) Rauschenbach, S.; Vogelgesang, R.; Malinowski, N.; Gerlach, J. W.; Benyoucef, M.; Costantini, G.; Deng, Z.; Thontasen, N.; Kern, K. *ACS Nano* **2009**, *3*, 2901.
(22) Dougherty, D. B.; Jin, W.; Cullen, W. G.; Reutt-Robey, J. E.; Robey, S. W. *J. Phys. Chem. C* **2008**, *112*, 20334.
(23) Jiang, N.; Zhang, Y. Y.; Liu, Q.; Cheng, Z. H.; Deng, Z. T.; Du, S. X.; Gao, H. J.; Beck, M. J.; Pantelides, S. T. *Nano Lett.* **2010**, *10*, 1184.
(24) Pettinger, B.; Ren, B.; Picardi, G.; Schuster, R.; Ertl, G. *J. Raman Spectrosc.* **2005**, *36*, 541.

(25) Wustholz, K. L.; Henry, A.-I.; McMahon, J. M.; Freeman, R. G.; Valley, N.; Piotti, M. E.; Natan, M. J.; Schatz, G. C.; Van Duyne, R. P. *J. Am. Chem. Soc.* **2010**, *132*, 10903.
(26) Dieringer, J. A.; Lettan, R. B.; Scheidt, K. A.; Van Duyne, R. P. *J. Am. Chem. Soc.* **2007**, *129*, 16249.
(27) McCreery, R. L. *Raman Spectroscopy for Chemical Analysis*; Chemical Analysis Monograph Series, Vol. *157*; Wiley: New York, 2000.
(28) Sonntag, M. D.; Chulhai, D.; Seideman, T.; Jensen, L.; Van Duyne, R. P. *J. Am. Chem. Soc.* **2013**, *135*, 17187.